Valcárcel-Germes, M.; Ibañez, G.; Martí-Renau, R.; Beltran, J.; Cebolla Cornejo, J.; Rosello Ripolles, S. (2021). Optimization of electronic nose drift correction applied to tomato volatile profiling. Analytical and Bioanalytical Chemistry. 413(15):3893-3907. https://doi.org/10.1007/s00216-021-03340-5

Optimization of electronic nose drift correction applied to tomato volatile profiling

Mercedes VALCÁRCEL[a], Ginés IBÁÑEZ[b], Raúl MARTÍ[a], Joaquín BELTRÁN[c], Jaime CEBOLLA-CORNEJO[a], and Salvador ROSELLÓ[b]*

[a]*Joint Research Unit UJI-UPV - Improvement of agri-food quality. COMAV. Universitat Politècnica de València, Cno. de Vera s/n, 46022 València, Spain*

[b]*Joint Research Unit UJI-UPV - Improvement of agri-food quality. Agricultural Sciences and Natural Environment Department, Universitat Jaume I, Avda. Sos Baynat s/n, 12071 Castelló de la Plana, Spain*

[c]*Reserach Institute for Pesticides and Water (IUPA) , Universitat Jaume I, Avda. Sos Baynat s/n, 12071 Castelló de la Plana, Spain*

**Corresponding author: E-mail: rosello@uji.es. Postal address: Universitat Jaume I, ESTCE, Avda. Sos Baynat s/n 12071 Castellón de la Plana.*

M. Valcárcel ORCID no.: 0000-0002-9347-1500
G. Ibañez ORCID no.: 0000-0002-1787-8587
R. Martí ORCID no.: 0000-0002-3517-1948
J. Beltran ORCID no: 0000-0003-4387-101X
J. Cebolla-Cornejo ORCID no.: 0000-0002-2607-9920
S. Roselló ORCID no.: 0000-0002-7733-4178

Funding

This research was partially funded by Jaume I University with projects P1-1B2011-41 and COGRUP/2016/04. G. Ibáñez thanks Universitat Jaume I for funding his pre-doctoral grant (PREDOC/2015/45).

Abstract

E-noses can be routinely used to evaluate the volatile profile of tomato samples once the sensor drift and standardization issues are adequately solved. Short-term drift can be corrected using a strategy based on a multiplicative drift correction procedure coupled with a PLS adaptation of the Component Correction. It must be performed specifically for each sequence, using all sequence signals data. With this procedure, a drastic reduction of sensor signal %RSD can be obtained, ranging between 91.5% and 99.7%for long sequences and 75.7% and 98.8% for short sequences. On the other hand, long-term drift can be fixed up using a synthetic reference standard mix (with a representation of main aroma volatiles of the species) to be included in each sequence that would enable sequence standardization. With this integral strategy, a high number of samples can be analyzed in different sequences, with a 94.4% success in the aggrupation of the same materials in PLS-DA two-dimensional graphical representations. Using this graphical interface e-noses can be used to developed expandable maps of volatile profile similitudes, which will be useful to select the materials that most resemble breeding objectives or to analyze which preharvest and postharvest procedures have a lower impact on the volatile profile, avoiding the costs and sample limitations of gas chromatography.

Keywords: electronic nose, drift correction, chemometrics, sequence standardization, tomato.

Introduction

The objective evaluation of flavor in crops such as tomato is expensive and time-consuming, consequently, this trait has been usually disregarded. Today it is known that one of the main factors under the loss of flavor relies on the loss of alleles related to the contents of aroma volatiles [1], and the use of delayed ripening genes that alter the aroma profile, an effect that depends on the genetic background [2]. Additionally, tomato flavor can also be altered by the preharvest and postharvest management of the crop that also alter the production of volatiles [3 – 6], .

In order to satisfy the demands of high quality markets, it would necessary to include flavor evaluation, and especially the volatile profile, during the development of breeding programs [7], cultivation, and postharvest procedures. In this context, the use of trained panelists or the precise volatile quantifications by gas chromatography-mass spectrometry is discarded considering that these evaluations are too expensive and time-consuming and, consequently, not adequate to evaluate a high number of samples.

As an alternative, electronic noses (e-noses) were designed to evaluate the volatile profiles of agricultural products [8]. For this purpose, they have been usually applied to classify materials considering their quality characteristics, their origin, the variety or the presence of diseases, additives, adulterations, and off-flavors in different fruits and vegetables (tomato, kiwifruits, peach, nectarine, apple, banana, persimmon, grape, watermelon, strawberry, blackberry, onion, potato, pumpkin, broccoli, etc.), grains (wheat, rice, maize, peanuts, etc.), aromatic and medicinal plants (tea, coffee, saffron, cocoa, oregano, ginseng, etc.), processed products (oils, juices), livestock and poultry meat, and fish [8–12]. Most of these applications were modeled and tested in a short-term scenario, using a limited number of samples. However, the application of this technology to the evaluation of materials in breeding programs and food industry makes it is necessary to assure the capability to process a high number of samples in the same day, as well as being able to compare them with data obtained in previous assays. By doing so, it would be possible to apply e-noses to selection and quality control programs, in which each new sample is compared with reference

values or fingerprints obtained in previous assays with elite materials grown and handled in ideal conditions. From this point of view, the objective would not be centered on classifying a new sample, but to have an idea of its distance to elite reference samples. Consequently, it would be possible to select the best individuals or those preharvest or postharvest procedures that minimize their impact on the volatile profile.

In order to take advantage of the capabilities of e-noses, it would be necessary to overcome the effects of sensor drift. This phenomenon is defined as temporary or gradual changes in one or some sensor properties which causes distorted response measures and reduces the validity of the electronic fingerprints. It is inevitable and caused by complex and dynamic processes, such as changes in room environmental conditions (temperature or humidity), changes in the composition of measured samples (component interactions), instrument operational disturbances (sensors thermal and memory effects, aging or poisoning) [13, 14]. These changes can be noticed both, in signals within a work sequence (short-term drift) and signals obtained in different work sequences (long-term drift). The improvement of sensor technology at the manufacturing stage to enhance its stability over time has contributed to reduce these problems. However, despite the advances obtained, a regular calibration is still required to limit the effects of sensor drift. It can be performed using external standards and statistical multivariate calibration models. Nonetheless, multivariate calibration requires a large number of samples and frequent re-calibrations of the sensor arrays and this would limit the number of new samples analyzed. Therefore, a new model calibration transfer or update and signal standardization using only a small number of reference samples would represent an interesting solution to keep the system operative for long periods [14].

In the last two decades, an enormous research effort has been made on different methodologies aimed to properly process signals and data from e-noses (reviewed by [13–15]). Nevertheless, it seems clear that, despite the high amount of research on drift correction and calibration update methods developed, these proposals were not routinely used, except for component correction and directed standardization methods. The best solutions proposed up to now rely on the analysis of a

high number of samples to develop robust models or use simple volatile mixes. These approaches are distant from the real context of tomato evaluation. This species has a complex volatile profile with more than 400 compounds, with nearly 30 of them playing an important role in tomato aroma perception [2]. On the other hand, the need to develop models with a high number of samples would not be realistic in high-throughput evaluations, as the models would have to be recalculated each time a sensor has to be changed.

In this context, although the use of commercial electronic noses for the evaluation of volatile profiles has a huge potential, it is necessary to develop an operating methodology enabling the routine evaluation of wide collections of real samples. This is, in fact, the aim of this paper, to propose a practical methodology to correct drift within and between sequences, using a minimum number of samples to calibrate the models and a tomato-like complex synthetic reference mix to standardize sequences. Finally, the development of long-term expandable partial least squares discriminant analysis (PLS-DA) graphical maps of e-nose volatile profiles is proposed as a valuable tool to enable the routine evaluation of the volatile profile of new samples, analyzing the relative distance to reference points.

Materials and Methods

Plant material and tomato-like synthetic standards

Tomato-like synthetic standards were developed to obtain a synthetic mixture of main volatile compounds of an average real tomato sample, but with higher stability and reproducibility. For this purpose, a high concentration standard mixture was prepared (TomSSt_4), containing 30 individual volatile compounds at concentrations (Table 1) corresponding to the mean values of representative tomato cultivars with different aromatic profiles [16]. Three alternative standards were obtained diluting TomSSt_4 to 70% (TomSSt_3), 50% (TomSSt_2) and 30% (TomSSt_1). The dilutions were obtained to cover a wide range of volatile sample concentrations. TomSSt_2 was employed

as a reference sample for inter-sequence standardization in long-term drift correction. These working solutions where prepared by volume dilution from more concentrated stock solutions which were stored in the freezer at -30ºC in sealed vials. They have an established stability of one year for the main stock solutions (around 500 ppm or higher) and of 1 month for the ppb to sub ppm solutions. As preparation of synthetic standards is carried out by dilution in volume of stock standards, this process can be reliably and reproducibly performed producing adequate standard solutions in the routine laboratory. For sequences run in different months, the specific standard mixtures were prepared de novo to provide restrictive conditions.

Table 1

Composition of the tomato-like synthetic standard TomSSt_4.

Volatile compound	ng mL^{-1}	Volatile compound	ng mL^{-1}
E-2-hexen-1-ol acetate	0.70	eugenol	13.92
3-methyl thiopropanal	1.12	nonanal	11.12
terpineol (alpha+beta+gamma)	0.56	2-isobutylthiazole	26.40
E-2-hexen-1-ol	1.10	E-2-heptenal	24.96
1-hexanol	2.02	methyl salicylate	892.00
3-carene	2.11	guaiacol	480.00
3-methylbutyl acetate	2.04	E-2-hexenal	702.00
alpha-pinene	1.98	6-methyl-5-hepten-2-one	590.00
gamma-terpinene	2.08	hexanal	800.00
2-carene	7.20	Z-3-hexenal	824.00
linalool	6.60	E-2-octenal	102.00
phenylacetaldehyde	9.20	citral (Z+E)	170.40
2-phenylethanol	12.04	R-limonene	98.00
6-methyl-5-hepten-2-ol	13.64	Z-3-hexen-1-ol	216.80
beta-ionone	13.16	geranyl acetone	114.80

Tomato varieties evaluated in this work represented a wide diversity of fruit shapes, colors, genotypic structures (commercial hybrids and landraces), and origins (Table 2). The plant material included four commercial hybrids, “Zayno RZ”, “Divyne RZ”, “Vinchy RZ” (Rijk Zwaan Iberica, Almería, Spain), and “Caramba” (De Ruiter Seeds, Almería, Spain). Four experimental tomato breeding lines (UJI008, UJI011, UJI014, and UJI028) with different fruit sizes. One cherry tomato type accession (BGV004587). Five accessions of local landraces, UJI023 of “de penjar” landrace, BGV005477 accession of a “Morado” landrace, BGV005651 an accession of “Muchamiel” landrace, BGV005718 an accession of “Amarillo” landrace, and BGV005655 an accession

belonging to the "Valenciano". The "de penjar" landrace carries with *alcobaça*, *alç*, long-life mutation allelic to the *nor* gene [17] and it results in a very specific aroma volatile evolution [18], "Morado" landrace has external pink color due to the transparent peel typical of the *yellow*, *y,* mutation which alters the synthesis of polyphenols and "Amarillo" has yellow flesh color typical of the impairment of carotenoid synthesis resulting from the presence of the *yellow-flesh*, *r*, mutation (reviewed by [19]) and it, therefore, affects the synthesis of apocarotenoid volatiles.

UJI accessions were obtained from Universitat Jaume I and BGV accessions from the genebank of the Instituto Universitario de Conservación y Mejora de la Agrodiversidad Valenciana (COMAV).

Table 2

Description of the tomato accessions tested in the different assays performed.

Code	Type of material	Accession	Number of sequences			Fruit characteristics
			1st assay	2nd assay	3rd assay	
1	Commercial hybrid	"Zayno RZ"[a,z]	3	1	3	Large, rounded, green-red
2	"Amarillo" landrace	BGV005718[b,x]	3	1	3	Large, slightly flattened, yellow
3	Commercial hybrid	"Caramba"[a,y]	1	1	1	Large, flattened, green-red
4	Breeding line	UJI011[c,u]	1	1	1	Large, rounded, red
5	Commercial hybrid	"Divyne RZ"[a,z]	1		1	Medium-large, rounded, red
6	Commercial hybrid	"Vinchy RZ"[a,z]	1		1	Large, rounded, red, long life
7	"De penjar" landrace	UJI023[b,u]	1	1	1	Small, rounded, red, long life
8	"Morado" landrace	BGV005477[b,x]	1	1	1	Large, slightly flattened, pink
9	"Muchamiel" landrace	BGV005651[b,x]	1	1	1	Large, flattened, red-orange,
10	"Valenciano" landrace	BGV005655[b,x]	1		1	Medium-large, heart-shaped, red-orange
11	Cherry tomato	BGV004587[b,x]	1		1	Small, rounded, orange-brownish
12	Breeding line	UJI008[c,u]	1		1	Small, rounded, red
13	Breeding line	UJI014[c,u]	1		1	Medium-large, slightly flattened, red
14	Breeding line	UJI028[c,u]	1		1	Small, rounded, red
TomSSt1	Tomato like standard (30%)		3		3	
TomSSt2	Tomato like standard (50%)		3	1	3	
TomSSt3	Tomato like standard (70%)		3		3	
TomSSt4	Tomato like standard (100%)		3		3	

Tomato types: [a]commercial hybrid, [b]local landraces, [c]breeding lines
Origin: [z]Rijk Zwaan Iberica S.A., [y]De Ruiter Seeds S.A., [x]Instituto Universitario de Conservación y Mejora de la Agrodiversidad Valenciana (COMAV) seed bank, [u]Univesitat Jaume I seed collection.

Experimental design

158 Three different assays were performed. In the first assay, 18 samples with different compositions
159 were used. These samples included real tomato samples from 14 varieties obtained homogenizing
160 whole fruits (Table 2) and the four tomato-like synthetic standards (TomSSt) with variable volatile
161 composition. Three sequences were run on different days. Each sequence included four specific
162 varieties (that were included only in one sequence) and two varieties that were included as controls
163 in the three sequences. The 4 tomato-like synthetic standards were also included in all the sequences.
164 Tomato samples were replicated 7 times and tomato-like synthetic standards 4 times in each
165 sequence. All the samples were randomly distributed in each working sequence.
166 For a deeper study of the short-term drift, a second assay was designed to include a higher number of
167 repetitions (12) per sample. Two consecutive long work sequences (22 hours each) were planned to
168 test seven tomato and one tomato-like synthetic standard (TomSSt_2). All the samples were also
169 randomly distributed within the first replicate of each sequence, and the order was maintained in the
170 rest of the replicates. This design provided data to compare the performance in a whole sequence (12
171 repetitions/sample in 22 hours) or a short sequence (4 repetitions/sample in 8 hours approximately)
172 to test the performance of the drift correction strategy proposed in different scenarios.
173 Finally, a third assay was performed to analyze the effect of long-term drift. To ensure the inclusion
174 of long-term drift in the signal responses, the sequences of this trial were carried out in a 3 months
175 period (one sequence per month) included in the normal routine usage of the equipment. During this
176 period other samples from tomato and other vegetable crops were analyzed in the equipment. The
177 short-term drift correction was applied before analyzing the results.
178 In a first step, the effect of long-term drift was analyzed using the four tomato-like standard solutions
179 in three sequences. Then the effect of long-term drift was also checked adding two tomato varieties
180 analyzed in three sequences. Long-term drift correction via sequence standardization was then
181 applied and its validity checked.
182 The independent study of each one of these three sequences was used to test and correct short-term
183 drift within a work-day sequence. The joint data of all these sequences were used to test the

184 performance of the long-term drift correction between sequences and standardization strategies
185 proposed in this work.
186 Once the reliability of the long term-drift correction had been checked it was applied to analyze the
187 data obtained from the analysis of the 14 tomato varieties distributed in three sequences, using the
188 data from TomSST2 for sequence standardization.
189
190 *Electronic nose and data acquisition*
191 A FOX 4000 (Alpha MOS, Toulouse, France) e-nose system was used. The system included 18
192 metal oxide semiconductor sensors (MOS) installed in three chambers, an autosampler system
193 (CombiPAL HS100, CTC Analytics, Zwingen, Switzerland), and a software package (AlphaSoft
194 v11) to control and process initial data. The sensor response in MOS sensors is a resistance variation
195 due to a reaction caused by the chemical species on the surface of the active layer of the sensor. As
196 usual for MOS sensors, the signal was expressed as normalized resistance variation of the signal
197 highest point $((R_i - R_{max})/R_i)$, where R_i is resistance at time zero and R_{max} is resistance in the signal
198 highest point of the sensor [20].
199 The analysis parameters related to general aspects of equipment operation were fixed following
200 manufacturer recommendations, while those that directly determine the response quality (influence
201 headspace generation) were established from previous tests based on the methodology for the
202 analysis of tomato aroma developed by the group [16]. For each sample, 2 g of homogenate (2 mL
203 in the case of tomato synthetic standards) were introduced into a 10 mL vial and sealed. Each sample
204 replicate corresponded to an independent vial. Samples were incubated in the autosampler at 45ºC
205 for 10 minutes to generate the headspace and then 2 mL of it were injected into the sensors chambers
206 for analysis. The sensors' response was recorded over two minutes with 18 minutes between each
207 measurement to allow the baseline recovery. Between samples, dry clean synthetic air flowed over
208 the sensor array for 2 minutes to remove residues of the previous sample, following manufacturer
209 recommendations. The gas flow rate was 150 mL min^{-1}. Instrument maintenance (daily auto test

and two-week diagnosis) were routinely performed following supplier protocols to ensure proper operation.

Drift correction and inter-sequence standardization

A multivariate adaptation of the multiplicative drift correction procedure proposed by Salit and Turk [21], combined with a partial least squares (PLS) adaptation of the component correction strategy [22] to model time-dependent drift was used both to remove intra-sequence short-term drift and to perform inter-sequence standardization to counteract long-term drift. Salit and Turk method is based on an interpolative projection of sample signal onto a smooth function defined by fitting to signals from regularly interspersed standards. Component correction strategy is based on the assumption that there is a subspace direction that captures only the drift variance and can be modelled (they use Principal Component analysis) and substracted from the measurement matrix X to provide drift corrected signals. Two assumptions were considered: i) drift, regardless of its type, is a function of time, and ii) drift for our electronic nose instrument is multiplicative (i.e. the magnitude of the perturbations is dependent on the signal level). Additionally, it had to be considered that the nature of the samples being analyzed could not be contemplated by the model, as they were unpredictable.

A practical guide of our proposed intra-sequence drift correction methodology is included in Supp. Fig. 1. According to [21], when multiplicative drift appears, the signal measured in a sample i evaluated with j repetitions in each of the k sensors of the system ($S_{i_{(j)},k\,\mathrm{measured}}$) could be decomposed as:

$$S_{i_{(j)},k\,\mathrm{measured}} = S_{i,k\,\mathrm{truth}}(1 + E_{\mathrm{drift}}(t) + E_{\mathrm{noise}}) \qquad (1)$$

Being $S_{i\,\mathrm{truth}}$ the true signal for sample i, $E_{\mathrm{drift}}(t)$ the drift estimation as a function of time and E_{noise} the estimation of the background noise (independent of time). $S_{i\,truth}$ can be estimated using the mean of all $\hat{S}_{i,k\,\mathrm{measured}}$

Then the multiplicative deviation pretreatment for each measured signal ($\frac{S_{i_{(j)},k\ \text{measured}}}{\hat{S}_{i,k\ \text{measured}}}$) allowed to model the deviations from 1 as an estimate of $E_{i,k\ \text{drift}}\ (t) + \ E_{i,k\ \text{noise}}$

To estimate time-dependent drift, a multivariate PLS regression between the pretreated signal measurements for all system sensors as independent variables (X matrix) and the time of analysis as a dependent variable (Y vector) was performed. As PLS drift model finds latent variables that explain the variability in the deviation of electronic signals due only to time evolution, this model function provides the estimate of $E_{i,k\ \text{drift}}\ (t)$ and the residuals of these model provide the estimation of $E_{i,k\ \text{noise}}$.

Accordingly, as proposed by [22], after the drift model was fitted, the matrix product of resulting loadings and scores of the model was used to calculate the matrix of $E_{\text{drift}}\ (t)$ components. Then the initial signal measured values were corrected for multiplicative drift using the following equation from [21]:

$$S_{i_{(j)},k\ \text{corrected}} = [\hat{S}_{i,k\ \text{measured}}(1 - \ E_{i_{(j)},k\ \text{drift}}\ (t))] + \ S_{i_{(j)},k\ \text{measured}} \quad (2)$$

A similar strategy was used to perform inter-sequence standardization to correct long-term drift. A practical guide is included in Supp. Fig. 2. For different work sequences, a generalization of equation (1) was considered to decompose signal measured in a sample *i* evaluated with *j* repetitions in each of the *k* sensors of the system. This generalization assumes that in this case the truth signal can be estimated using two components, the mean of all $S_{i_{(j)}}$ repetitions and an inter-sequence standardization coefficient. To calculate this inter-sequence standardization coefficient, the difference of the signals of the same reference sample measured in two different sequences was used. The tomato-like standard TomSSt_2 was used as a reference sample in all work sequences. Consequently, the multiplicative deviation pretreatment used for each measured signal was:

$$\frac{S_{i_{(j)},k\ \text{measured}}}{\hat{S}_{i,k\ \text{measured}} + (\hat{S}_{\text{TomSSt1},k} - \hat{S}_{\text{TomSStn},k})} \quad (3)$$

Where $\hat{S}_{TomSSt1,k}$ and $\hat{S}_{TomSStn,k}$ are the signal means of all repetitions for the tomato-like synthetic standard reference sample in sequences 1 and *n*, respectively, for each *k* sensor.

The generalization of equation (1) also assumes that, when considering several work sequences, the time-dependent drift can be decomposed in two components:

$$E_{\text{drift}}(t) = E_{\text{short}}(t) + E_{\text{long}}(t) \quad (4)$$

Where E_{short}(t) represents the short-term (between-sample within-run) signal drift and E_{long}(t) the long-term (between-run) drift. Inter-sequence standardization was applied to all sequences after short-drift correction. Doing that, time-dependent drift would be equivalent to the long-term drift that appears between sequences. Consequently, after applying pretreatment of equation (3) when drift was modeled by PLS regression as explained previously, it was possible to calculate the matrix of E_{long} components and to use it to standardize sequence signals applying equation (4).

The PLS regressions were performed using venetian blinds (with as many groups as samples evaluated) as resampling procedure, in order to calculate error models and to select the number of latent variables used in the model. Outliers were detected and removed, using Hotelling T^2 and Q Residuals [23].

Graphical maps and data analysis tools

Drift-corrected sensor signals were graphically plotted in a 2D PLS-DA scatterplot map as with this dimensional reduction representation technique the distance between projected points preserves sample similarities [24]. Confidence ellipsoids (p=0.05) were calculated and plotted for samples with more than four replicates. In some cases, after removing outliers there were not enough points to calculate these intervals, and data points were just linked with lines to provide rapid identification of groups. The closer the points, the higher the similarity between signals. This procedure enables the comparison of sample volatile profile similarities, for example, for selection purposes. The objective was not to classify samples in predefined groups. This would be a typical objective in a quality assurance control, but in breeding programs, the objective is to select those materials closer to specific volatile profile targets. Nevertheless, to assess the performance of the proposed drift correction strategy, classification results were compared with those obtained using other reputed

drift correction methods: the original method proposed by Salit and Turk [21], independent component analysis (ICA) and parallel factor analysis 2 (PARAFAC2) [25]. ICA is a signal processing method that separates a multivariate signal into additive subcomponents assuming that the subcomponents are non-Gaussian signals and that they are statistically independent from each other. PARAFAC methods are generalizations of Principal Component Analysis (PCA) to higher order arrays. PARAFAC2 is an improvement of the original PARAFAC method in which the strict trilinearity is no longer required. Compared with PCA methods, PARAFAC methods have the advantages of no rotation problem, as in PCA, easier to interpret and higher statistical robustness.

Once the correction was obtained, three frequent classification techniques were applied. K nearest neighbors (KNN) classification, soft independent modeling of class analogy (SIMCA), and discriminant analysis based on partial least square regression (PLS-DA) [24] . KNN is a non-parametric classification method in which a data point is assigned to the class most common among its k nearest neighbors. SIMCA classification is mainly based on principal component analysis and an object is assigned to a class if its residual distance is below the statistical limit for the class. In PLS-DA, the predictive modelling comprises two main procedures, a PLS component development (i.e. dimension reduction for selecting variables for classification) and a prediction model construction (i.e. discriminant analysis) to predict class assignment for the data.

KNN, SIMCA, PLS and PLS-DA, analysis and graphics were performed using PLS_Toolbox v 8.6 (Eigenvector Research Inc, Wenatchee, WA, USA) for Matlab v 9 (Mathworks Inc, Natick, MA, USA). ICA models [26] were calculated with the FastICA toolbox for Matlab developed at the Helsinki University of Technology. PARAFAC2 models were performed using a graphical user interface, SENSABLE [20].

To justify the need for standardization procedures, tests for significant differences between the same sample signals in different sequence work using MANOVA analysis and Roy test were used [24]. These analyses were performed using IBM SPSS v.24 (IBM Corp., Armonk, NY, USA).

Results and discussion

Short-term drift correction

In the first assay, high levels of short-term drift were observed leading to a high variation in the position of each sample replicate in the two-dimensional representation of the PLS analysis obtained with raw signals (Fig. 1 a, b, and c). This variation could be related to a possible lack of homogeneity of real tomato samples, but a considerable variability was also detected in tomato-like standards which are highly homogeneous. As a consequence, despite having a different aroma volatile profile, the confidence ellipsoids of each variety overlapped. Thus, it was impossible to discriminate the materials. This effect of short-term drift was detected in the three independent sequences tested, but it affected each sequence differentially. As an example, the confidence ellipsoid of the tomato-like standard TomSSt_2 was small and data points plotted close in the first sequence (Fig. 1a), while the ellipsoid was considerably wider in the second (Fig.1b) and third sequences (Fig. 1c). The contrary was observed in the case of TomSSt1, with higher variability in the first sequence and lower in the second and third. As the samples were randomly distributed for each replicate in the sequence, the differences observed in confidence ellipsoids suggest that the effect of drift changes between sequences. This spurious trend confirmed the difficulty of extrapolating short-term drift effects on different analysis sessions.

The effect of sequence duration on short-term drift was analyzed in-depth comparing the performance of long (22-hour) and short (8-hour) sequences using 8 samples, including 7 tomato varieties and one tomato-like standard (Table 2). This time, samples were randomized in the first replicate, but the order was maintained in the rest of the replicates to enable comparisons between varieties. The long sequence (22 hours), typical of situations where a high number of samples is to be analyzed, was obtained increasing the number of repetitions per sample up to 12. Raw sensor data from these analyses revealed, for all the samples and in all the sequences, the presence of an important drift effect that affected all the sensors. The drift affected differentially each variety, with the highest effects detected in the samples of the variety “Caramba” (Fig. 2).

These drift effects were more evident and important at the end of the sequence (Fig. 2a), showing a complex non-linear time-dependent variation, with positive and negative signals tending to converge to 0. In the case of "Caramba" samples, raw signals (12 repetitions distributed in a sequence of 60 analysis) showed a very high relative standard deviation (%RSD) for the complete sequence for all the sensors (Fig. 2b. first data in parenthesis).

In order to provide a reference, these values obtained with "Caramba", were compared to those obtained by Xu et al. [27] corresponding to 6 analyses with the same apparatus equipped with the same sensors (Fig. 2b in square brackets). %RSD values obtained in the present work were considerably higher. Thus, the use of long sequences such as these would be unacceptable. It should be considered though, that the material used by [27] was *Semen arecae*, a dried seed preparation from *Areca catechu* L. Therefore, differences in %RSD would be explained both by changes in the sample matrix and in the number of hours of work of the sensors per sequence.

When shorter sequences were considered (8 working hours, i.e. 4 "Caramba" samples distributed in a sequence of 18 injections) the drift levels were lower, but they continued to be excessive (Fig. 2d. first data in parenthesis).

The main factors contributing to e-nose drift effects in sensor performance are usually due to differences in temperature, humidity, changes in samples analyzed due to components interactions, or other uncontrolled effects. In the long term, the stability of MOS sensors could progressively be affected by sensor aging or poisoning affecting their performance. This includes changes in the morphology of the sensing layer and irreversibly bind of some sample compounds to metal oxides which diminish the catalytic oxidation of sample volatiles and affecting the sensors' resistance response [14]. In practice, the data distortion caused by sensor drift in short time scenarios (one or few work-sequences) has many times been avoided when the use of the data collected was strictly for classification purposes. In these cases, the use of advanced multivariate statistical classification methodologies makes it possible to obtain subjacent information from the raw signal characteristic of each sample group, discarding the rest of the signal information and thus diminishing the drift

364 distortions problems (see examples in [28–30]). Unconsciously, when using a multivariate
365 classifying technique, the analysis identifies and, to preserve sample group characteristic
366 information, it discards the "non-characteristic" part of raw sensor signal which is normally related
367 to noise, drift, and other non-relevant information. Nevertheless, this "signal cleaning" is a
368 collateral effect (unwanted effect) and, consequently, the success of this strategy is variable since
369 the characteristic subjacent information of the group is highly dependent on the samples and the
370 number of latent variables used to build up the classification model. When a reduced number of
371 samples with important differences between them are evaluated or when the volatile composition
372 of the samples is not complex the "signal cleaning" effect would work well, making it possible to
373 classify the samples in a quite satisfactory way [31]. But, with this approach, it is not always
374 possible to completely avoid drift distortion effects. It would be the case of complex samples
375 (complex matrix and/or very complex mixtures of volatiles) or collections of samples with similar
376 volatile profiles. Consequently, a drift correction strategy would be more convenient in those cases.
377 In order to correct short-term drift effects, sensor drift of the second assay was modeled and
378 subtracted from the raw signals. To do that, a multivariate adaptation of the multiplicative drift
379 correction procedure proposed by Salit and Turk [21] combined with a PLS adaptation of the highly
380 used component correction strategy [22] to specifically model each drift present in each sequence
381 was performed. The following assumptions were considered: i) sensors of the array have similar
382 drift behavior, ii) this drift has a specific direction in the data hyperspace which allows its
383 modelization by regression, and iii) this drift is time-dependent. After modeling short-term drift for
384 each sequence, drift components for each signal in the data matrix were calculated. Later, matrix
385 subtraction was performed in a Matlab environment to remove drift from the raw sensor signal data,
386 thus providing a corrected sensor data matrix, which was used to plot the data (Fig. 2e). Compared
387 with the raw sensor signals (Fig. 2a), the corrected signals were much more stable during the whole
388 sequence for all sensors, even those with higher %RSD. Accordingly, an impressive %RSD
389 decrease was observed for all the sensors (Fig. 2b), ranging from between 91.5% and 99.7% for

390 long sequences and 75.7% and 98.8% for short sequences. Maximum %RSD values were 0.65%
391 for long sequences and 0.72% for short sequences. Those values are were between one (T40/2
392 sensor) and 27 (LY2/LG sensor) times lower than those reported by Xu et al. [27] with a lower
393 number of injections. As expected, the use of shorter work-sequences (18 injections in 8 hours
394 sequence) resulted in better performance after drift correction (Fig. 2d and 2f), as it avoided the
395 higher levels of drift detected at the end of long sequences.
396 It should be considered though, that the increase in stability entailed a small decrease in the absolute
397 value of signals after correction. This side effect mainly affects long sequences (Fig. 2a vs. Fig. 2e),
398 while this decrease is imperceptible in shorter sequences (Fig. 2c vs. Fig. 2f). Consequently, despite
399 the powerful short-term drift correction capabilities obtained, it would be preferable to use short (8
400 hours) work sequences.
401 When this drift correction strategy was applied to the signals of the first assay, an impressive
402 reduction of the sample signal variability was attained, enabling a clear comparison of similitudes
403 between samples in the new PLS-DA similarity map obtained (corrected: Fig. 1d, 1e, and 1f vs.
404 raw: Fig. 1a, 1b, and 1c). Indeed, after this correction, it was easy to ascertain similarities in the
405 volatile signal profile between samples, and the confidence intervals did not overlap as it had
406 happened with the raw data.
407 The use of similitude maps to compare volatile profiles is a novel alternative. Therefore, in order
408 to compare this strategy with previous works it was necessary to assess its performance using
409 classification methodologies, which are rather popular in e-nose preceding literature. Consequently,
410 using the data of the second assay, the new drift correction strategy was compared with alternative
411 drift correction methods including the original approach by Salit and Turk, [21], ICA [32], using
412 KNN, SIMCA, and PLS-DA as classifying methods. In general, SIMCA outstood in the
413 classifications. KNN and PLS-DA had a similar performance, which varied depending on the
414 variety considered (Table 3). Considering different alternatives, the new correction proposed in this
415 work offered the best results (classification effectiveness) compared to the alternatives evaluated

416 independently of the classification method. In fact, SIMCA and KNN classification with the
417 proposed short-term drift correction allowed to classify correctly a 100% of the samples, assigning
418 them to the variety to which they belonged.

Table 3

Percentage of samples correctly classified using KNN (K=8), SIMCA and PLS-DA classification methods for seven tomato cultivars and the tomato-like synthetic standard 2, before (raw data) and after intra-sequence drift correction using the proposed correction based on an adaptation of [21] and PLS component correction method, the Salit and Turk [21], ICA [32] and PARAFAC2 [20] methods. Average data of three work-sequences is provided (variation range in brackets).

Sample	Raw data			Proposed correction			Salit & Turk correction			ICA correction			PARAFAC2 correction		
	KNN	SIMCA	PLS-DA	KNN	SIMCA	PLS-DA	KNN	SIMCA	PLS-DA	KNN	SIMCA	PLS-DA	KNN	SIMCA	PLS-DA
TomSSt_2[a]	98.9 (97.9-100)	100	100	100	100	100	97.6 (93.8-100)	56.3 (51.1-60.6)	100	94.8 (86.5-100)	100	93.8 (81.3-100)	99.0 (97.9-100)	100	93.7 (88.3-99.0)
Zayno	85.4 (78.6-92.9)	82.0 (49-99)	90.4 (84.7-100)	100	100	99.3 (98.0-100)	92.2 (83.6-100)	60.1 (52-67.7)	93.5 (88.7-100)	83.6 (76.5-91.8)	96.6 (89.8-100)	80.9 (74.5-85.7)	80.3 (77.5-85.7)	81.6 (72.4-89.6)	72.7 (66.3-80.6)
"Amarillo" (BGV005718)	91.5 (87.8-99.0)	98.3 (94.8-100)	88.4 (83.5-91.8)	100	100	94.6 (90.8-100)	99.7 (99.0-100)	57.9 (52.1-59.4)	89.7 (85.6-91.8)	79.9 (64.3-98.0)	98.3 (94.8-100)	83.3 (76.5-87.8)	86.4 (74.4-93.9)	88.4 (85.7-90.6)	68.5 (55.1-80.6)
Caramba	60.5 (47.9-84.7)	76.5 (69-89.8)	76.8 (68.0-83.7)	100	100	94.5 (92.9-98.0)	89.0 (82.6-92.9)	52.4 (51-54.1)	80.8 (78.3-85.6)	54.8 (47-62.2)	76.5 (70.8-89.8)	81.3 (61.2-91.7)	66.8 (62.7-69.3)	64.9 (56.3-71.4)	60.5 (48.4-71.0)
Breeding line (UJI011)	78.2 (71.4-82.6)	79.8 (68-90.8)	77.7 (70.8-83.7)	100	100	92.4 (82.2-100)	94.2 (90.8-99.0)	53.8 (53.1-55.2)	78.3 (69.9-86.7)	63.6 (55.1-76.5)	83.2 (68-90.8)	65.2 (61.2-67.3)	61.2 (52-71.4)	67.5 (53.1-79.6)	67.9 (61.2-73.5)
De penjar (UJI023)	96.3 (91.8-99.0)	100	99.7 (99.0-100)	100	100	100	96.5 (90.6-100)	60.7 (56.1-65.6)	97.2 (91.7-100)	75.8 (56.1-86.6)	100	88.1 (71.4-100)	93.8 (90.6-98.0)	94.9 (89.8-98)	84.3 (81.6-89.8)
Morado (BGV005477)	88.8 (76.5-99.0)	100	92.8 (89.6-94.9)	100	100	98.0 (93.9-100)	97.3 (92.9-100)	72.4 (66.7-82.3)	94.5 (92.7-96.9)	79.2 (45.9-98.0)	100	90.1 (79.6-96.9)	95.2 (90.8-98.0)	91.5 (79.6-97.9)	85.3 (81.3-88.8)
Muchamiel (BGV005651)	82.8 (82.3-83.7)	96.9 (90.8-100)	77.9 (74.3-79.7)	100	100	95.9 (93.9-98.0)	91.4 (82.3-100)	57.8 (55.1-63.3)	84.3 (77.4-93.9)	79.7 (54.3-94.0)	96.9 (90.6-100)	83.7 (75.3-91.0)	85.8 (82.3-91.8)	93.2 (90.8-96)	77.9 (75.3-81.6)

Long-term drift and sequence standardization.

Once the problem of short-term drift was solved, the focus was set on the effects of the variability detected among sequences. This variability, as stated above, can be generated by different causes originating a long-term drift effect. A solution to this effect is critical when a high number of samples are to be analyzed, as samples have to be distributed in different sequences that would be run on several days.

Regardless of the cause of inter-sequence variability, the effects can be considerable and unpredictable, as was pointed out in the comparison of the three sequences of the first assay. Consequently, it seemed clear that some reference samples should be included in each sequence to assess how long-term drift affected the signal. At this point, it would not be advisable to use real tomato samples as references. The storage capability of these samples would be limited, and long-term evolution in a freezer would introduce an undesirable noise in the system, thus increasing long-term drift. Accordingly, it was decided to include tomato-like synthetic standard volatile solutions, which were designed and created for this purpose. As tomato volatile profile is highly complex, with more than 400 volatiles being involved, it was decided to focus on a group of compounds (Table 1) that had been suggested to hold a prominent role in the aroma perception [33, 34]. Standards were created from stock solutions for each session. Nonetheless, in the future and for practical reasons, standards can be created and stored in sealed vials at -30°C during one month with a high stability. In this case, over a 3-month span, the standards were created specifically for each session, thus providing more restrictive conditions.

In a first step, three different sequences with the tomato-like standards at different concentrations were run. After applying the proposed short-term drift correction, a PLS-2D map was obtained (Fig. 3a). Samples from the same tomato-like standard tended to group together, but still, a considerable level of variation was detected. In some cases, the confidence intervals of the same samples run in different sequences did not overlap and intervals of different standards did overlap in one case.

Considering the homogeneous nature of these standards, this variability would not be mainly related with the nature of the sample. To check this point, the analysis was repeated including samples from two tomato varieties "Rayno RZ" and "Amarillo". Again, wide variability was detected, which was not specifically higher in the real tomato samples than in the standard solutions, despite their more complex nature (Fig. 3b).

This time, even in the case of the control with lower variability (TomSSt_1), the fluctuations of signal values were rather high for some sensors, reaching RSD values above 20% (e.g. LY2/gCTl and LY2/GH sensors) or very close to this threshold (e.g. LY2/G sensor). In fact, a MANOVA analysis for TomSSt_1 using the data from the three sequences showed significant inter-sequence differences (Roy test $\alpha < 0.03$). Higher levels of variation were found in the rest of the controls. Consequently, despite the use of the routine instrument calibration recommended by the equipment manufacturer, the unacceptable inter-sequence variance for each sample caused important bias in the graphs constructed joining the data from several sequences. Therefore, it makes necessary the use of a data standardization step before merging data from different sessions.

In order to tackle this long-term drift effect, the data from the tomato-like synthetic standard TomSSt_2 was selected to standardize sequence signals. The use of a real sample as reference had to be discarded, as its volatile profile would evolve during their conservation and it would also have a finite nature. On the opposite, a homogeneous synthetic standard including main tomato volatiles, representing the complex nature of its aroma, can be generated expressly for each sequence.

Following this premise, in order to standardize sequences, sensor signals from each sample after short-term drift correction were transformed using the deviation observed between the corrected signals of the synthetic standard in the different sequences. Once the signals were transformed, they were related to a time vector using PLS regression. Time vector values were obtained adding the time of each analysis, including the different sequences consecutively.

New PLS-DA 2D maps were then obtained, and the efficiency of correction was evident (Fig. 3a

476 vs 3b). For five of the six controls no significant inter-sequence differences were found, and the
477 confidence ellipsoids overlapped. Only in the case of the samples of the tomato landrace "Amarillo"
478 (coded 2_1 in Fig. 3) significant differences (Roy test $\alpha < 0.001$) were found between the first
479 sequence and the remaining two. Nonetheless, the three samples plotted at a short distance. The
480 standardization procedure showed a grouping correction efficiency of 94.4%, as 17 of the 18 sample
481 groups were correctly ascribed with their equals ran in different sequences and their confidence
482 intervals overlapped. This result represents a similar efficiency compared to other strategies
483 regarding long-term drift counteraction methods [15, 35–40] or better [41, 42]. It was confirmed,
484 then, that data from different sequences could be pooled in order to work with a high number of
485 samples.

486 Considering the good performance obtained with these controls, the sequence standardization
487 procedure was applied to the data obtained with three sequences, with 14 tomato varieties and
488 TomSSt_2 as a reference. When both short-term drift correction and sequence standardization was
489 applied (Fig. 4b), the variation observed per sample was highly reduced compared to the use of raw
490 data (Fig. 4a). Again, the replicates analyzed in different sequences tended to overlap their
491 confidence intervals, and only one of the replicates of the "Amarillo" landrace could not be grouped
492 with the rest of the corresponding replicates (coded 2.1 in Fig 4b). Therefore, this procedure enables
493 a realistic comparison of similitudes and differences in the volatile signal profile between samples
494 run in different sequences.

495 Other works [15, 35, 41] deal with adaptations of the component correction strategy applied to a
496 long-term drift counteraction. These works use a group of training samples to model the drift using
497 different regression methodologies (PLS, OSC, or CPCA) and, then subtract the drift modeled from
498 the signals of new samples. These strategies assume that with a good training set, the calibration
499 model can be useful for a long time for practical purposes. However, it is obvious that to extend the
500 period of use, large training sets are needed. Gutierrez-Osuna [43] used a training set of 5 to 10

501 samples for a drift correction period of 3 months in samples of 4 very different spices. Padilla et
502 al., [35] used training sets higher than 100 samples for a drift correction period of 10 months in
503 samples of individual chemical compounds at different concentrations. A similar application was
504 tested by Ziyatdinov [41] with training sets higher than 1000 samples for a drift correction period
505 of 7 months. Nevertheless, it seems also obvious that when sensor degradation increases, the
506 usefulness of these calibration models will decrease and, at any moment, they would need an
507 update. Additionally, training sets have been used with mixes of a few volatiles, and real tomato
508 samples consist of more than 400 volatiles [34].

509 In the present study, specific training set samples were not used. Instead, the information of the
510 samples evaluated in each sequence was used to calculate the specific drift correction model. Four
511 injections per sample would be enough to model short-term drift and at the same time providing a
512 reliable confidence interval. By doing so, each sequence would have its proper model and,
513 consequently, it would always be up to date. The unpredictable nature of short-term drift in different
514 sequences using tomato matrices would limit the efficiency of other alternatives.

515 On the other hand, the use of one reference synthetic standard has proven to be highly efficient to
516 standardize sequences in order to reduce inter-sequence variability, enabling the comparison of
517 samples analyzed in different sequences. This strategy would also be useful when a replacement of
518 sensors is performed or when different instruments are used to enlarge the processing capabilities
519 of the lab. Tomic et al., [37] tried a similar component correction strategy based on PCA and
520 complemented with multiplicative drift correction to accomplish a successful calibration transfer
521 between instruments. Other calibration transfer strategies which use sophisticated correction
522 methods and algorithms have been also applied to the expansion of calibration update models [38,
523 39, 44] but they need a higher number of training samples (10 to more than 400 depending on the
524 methodology) and were tested only for the detection of individual chemical compounds, so the
525 efficiency in more complex samples still needs to be tested [14].

526 Combining short-term and sequence standardization and PLS-DA 2D similitude maps it is possible
527 to easily identify differences in the volatile signal profiles of the samples. It is then possible to make
528 rapid identification of those samples with a volatile profile more similar to high quality reference
529 materials. This procedure would enable the use of e-noses for example in breeding programs. It
530 would be possible to select which genetic backgrounds have a lower negative impact on the aroma
531 profile. From an agronomic point of view, it would also enable a rapid identification of which
532 preharvest and postharvest procedures have the lowest impact on the volatile profile. These maps
533 would be expandable, offering the possibility of including new reference points. In fact, when Fig.
534 3c and 4b are compared, the relative position of the real tomato samples of "Zayno RZ" (coded 1
535 in the figures) and the "Amarillo" landrace (coded 2 in the figures) were not altered.

536 In the present work, this strategy has been successfully applied to a combination of different tomato
537 materials, selected to represent a wide variability of volatile profiles, especially in the case of tomato
538 landraces. The landraces included in the study had already shown a clearly different volatile profile
539 [45], and especially important as they are frequently commercialized in quality markets in which
540 consumers are willing to pay a price premium for excellent flavor [46]. Interestingly, "Muchamiel",
541 which had previously shown a less intense volatile profile in gas chromatography analysis
542 compared to "Valenciano" and "Morada", plotted in the PLS-DA 2D map in an area corresponding
543 to materials with lower volatile concentration (Fig.4b). The next step in future works will be
544 centered on the comparison of the volatile profile obtained with the e-nose and GC-MS data in
545 order to confirm this trend.

546

547 **Conclusions**

548 Short- and long-term drift compromises the application of e-noses to the evaluation of volatile
549 profiles. These effects are variable and unpredictable. Consequently, general models are not useful,
550 and the performance registered in each sequence has to be used in order to model drift effects. The

distribution of 4 replicates per sample and sequence enables the development of an effective and sequence-specific short-term drift correction. On the other hand, the unpredictable nature of the variation between sessions makes it necessary to use reference materials to standardize sequences. By doing so it would be possible to analyze a high number of samples distributed in different sequences. The use of a tomato-like synthetic has proven to be for this purpose. The two-step correction methodology proposed here, combined with PLS-DA two-dimensional similitude maps, will enable rapid and reliable identification of samples with a volatile signal profile similar to references selected as ideal targets.

Declarations

Funding

This research was partially funded by Jaume I University with projects P1-1B2011-41 and COGRUP/2016/04. G. Ibáñez also thanks Universitat Jaume I for funding his pre-doctoral grant (PREDOC/2015/45).

Conflicts of interest

The authors declare that there is no conflict of interest.

Availability of data and material

Data available on request to the authors

Code availability

Not applicable

Authors' contributions

Mercedes Valcárcel: Conceptualization, Methodology, Investigation, Formal analysis, Writing - Original Draft, and Supervision. Ginés Ibáñez: Formal analysis and Visualization. Raúl Martí: Formal analysis and Visualization. Joaquín Beltrán: Resources and Validation. Jaime Cebolla-Cornejo: Writing-Reviewing and Editing. Salvador Roselló: Conceptualization, Formal analysis, Writing - Original Draft and Supervision

577 **Ethics approval**

578 Not applicable

579 **Consent to participate**

580 All the authors have consented to participate on the research. The research does not include humans
581 nor animals as subjects of research.

582 **Consent for publication**

583 All the authors consent the publication of the research

584

585 **References**

586 [1] Tieman D, Zhu G, Resende MFR, Lin T, Nguyen C, Bies D, et al. A chemical genetic roadmap
587 to improved tomato flavor. Science. 2017; 355(6323):391–4; doi:10.1126/science.aal1556.

588 [2] Baldwin EA, Scott J, Shewmaker CK, Schuh W. Flavor trivia and tomato aroma: biochemistry
589 and possible mechanism for control of important aroma components. HortScience.
590 2000;35(6):1013–22; doi: 10.21273/HORTSCI.35.6.1013.

591 [3] Davies JN, Hobson GE. The constituents of tomato fruit — the influence of environment,
592 nutrition, and genotype. C R C Crit Rev Food Sci Nutr. 1981;15(3):205–80;
593 doi:10.1080/10408398109527317.

594 [4] Lahoz I, Pérez-de-Castro A, Valcárcel M, Macua JI, Beltrán J, Roselló S, et al. Effect of water
595 deficit on the agronomical performance and quality of processing tomato. Sci Hortic
596 (Amsterdam). 2016;200: 55-65; doi: 10.1016/j.scienta.2015.12.051.

597 [5] Schouten RE, Woltering EJ, Tijskens LMM. Sugar and acid interconversion in tomato fruits
598 based on biopsy sampling of locule gel and pericarp tissue. Postharvest Biol Technol.
599 2016;111:83–92; doi:10.1016/j.postharvbio.2015.07.032

600 [6] Boukobza F, Taylor AJ. Effect of postharvest treatment on flavour volatiles of tomatoes.
601 Postharvest Biol Technol. 2002;25(3):321–31; doi: 10.1016/S0925-5214(02)00037-6.

602 [7] Zhao J, Sauvage C, Zhao J, Bitton F, Bauchet G, Liu D, et al. Meta-analysis of genome-wide

association studies provides insights into genetic control of tomato flavor. Nat Commun. 2019; 10(1):1–12; doi: 10.1038/s41467-019-09462-w

[8] Loutfi A, Coradeschi S, Mani GK, Shankar P, Rayappan JBB. Electronic noses for food quality: A review. J Food Eng. 2015;144:103–11; doi:10.1016/j.jfoodeng.2014.07.019

[9] Kiani S, Minaei S, Ghasemi-Varnamkhasti M. Application of electronic nose systems for assessing quality of medicinal and aromatic plant products: A review. J Appl Res Med Aromat Plants. 2016;3(1):1–9: doi:10.1016/j.jarmap.2015.12.002.

[10] Sun Y, Wang J, Cheng S. Discrimination among tea plants either with different invasive severities or different invasive times using MOS electronic nose combined with a new feature extraction method. Comput Electron Agric. 2017; 143:293–301; doi: 10.1016/j.compag.2017.11.007

[11] Majchrzak T, Wojnowski W, Dymerski T, Gębicki J, Namieśnik J. Electronic noses in classification and quality control of edible oils: A review. Food Chem. 2018;246:192–201; doi: 10.1016/j.foodchem.2017.11.013.

[12] Jia W, Liang G, Jiang Z, Wang J. Advances in Electronic Nose Development for Application to Agricultural Products. Food Anal. Methods 2019; 12(10):2226-2240: doi: 10.1007/s12161-019-01552-1.

[13] Marco S, Gutierrez-Galvez A. Signal and data processing for machine olfaction and chemical sensing: A review. IEEE Sens J. 2012;12(11):3189–214; doi: 10.1109/JSEN.2012.2192920.

[14] Rudnitskaya A. Calibration Update and Drift Correction for Electronic Noses and Tongues. Front Chem. 2018; 6: 433; doi:10.3389/fchem.2018.00433/full.

[15] Gutierrez-Osuna R. Pattern analysis for machine olfaction: a review. Sensors Journal, IEEE. 2002;2(3):189–202; doi: 10.1109/JSEN.2002.800688.

[16] Beltran J, Serrano E, López FJ, Peruga a, Valcarcel M, Rosello S. Comparison of two quantitative GC-MS methods for analysis of tomato aroma based on purge-and-trap and on solid-phase microextraction. Anal Bioanal Chem. 2006; 385(7):1255–64; doi:

10.1007/s00216-006-0410-9.

[17] Casals J, Pascual L, Cañizares J, Cebolla-Cornejo J, Casañas F, Nuez F. Genetic basis of long shelf life and variability into Penjar tomato. Genet Resour Crop Evol. 2012;59(2):219–29; doi: 10.1007/s10722-011-9677-6.

[18] Roselló S, Nuez F, Casals J, Beltrán J, Casañas F, Cebolla-Cornejo J. Long-term postharvest aroma evolution of tomatoes with the alcobaça (alc) mutation. Vol. 233, Eur. Food Res. Technol. 2011. 233: 331–42; doi: 10.1007/s00217-011-1517-6.

[19] Cebolla-Cornejo J, Roselló S, Nuez F. Selection of tomato rich in nutritional terpenes. Natural Products: Phytochemistry, Botany and Metabolism of Alkaloids, Phenolics and Terpenes. 2013.

[20] Skov T, Bro R. A new approach for modelling sensor based data. Sensors Actuators, B Chem. 2005;106(2):719–29; doi: 10.1016/j.snb.2004.09.023.

[21] Salit ML, Turk GC. A drift correction procedure. Anal Chem [Internet]. 1998 Aug 1;70(15):3184–90; doi: 10.1021/ac980095b.

[22] Artursson T, Eklo T, Lundstro I, Sjo M. Drift correction for gas sensors using multivariate methods. J Chemom. 2000; 14 (5-6):711–23; doi: 10.1002/1099-128X(200009/12)14:5/6<711::AID-CEM607>3.0.CO;2-4.

[23] Ballabio D, Consonni V. Classification tools in chemistry. Part 1: linear models. PLS-DA. Anal Methods. 2013;5(16):3790; doi: 10.1039/C3AY40582F.

[24] Krzanowski W. Principles of multivariate analysis: A User's Perspective. Oxford University Press; 2000.

[25] Di Natale C, Martinelli E, D'Amico A. Counteraction of environmental disturbances of electronic nose data by independent component analysis. Sensors Actuators B Chem. 2002;82(2–3):158–65; doi: 10.1016/S0925-4005(01)01001-2.

[26] Hyvärinen a, Oja E. Independent component analysis: algorithms and applications. Neural Netw. 2000;13(4–5):411–30; doi: 10.1016/S0893-6080(00)00026-5

655 [27] Xu M, Yang SL, Peng W, Liu YJ, Xie DS, Li XY, et al. A novel method for the discrimination
656 of semen arecae and its processed products by using computer vision, electronic nose, and
657 electronic tongue. Evidence-based Complement Altern Med. 2015;2015. Doi:
658 10.1155/2015/753942
659 [28] Gromski PS, Correa E, Vaughan AA, Wedge DC, Turner ML, Goodacre R. A comparison of
660 different chemometrics approaches for the robust classification of electronic nose data. Anal
661 Bioanal Chem. 2014;406(29):7581–90; doi:10.1007/s00216-014-8216-7.
662 [29] Shi Y, Gong F, Wang M, Liu J, Wu Y, Men H. A deep feature mining method of electronic
663 nose sensor data for identification identifying beer olfactory information. J Food Eng. 2019;
664 263:437–45; doi:10.1016/j.jfoodeng.2019.07.023.
665 [30] Song J, Bi J, Chen Q, Wu X, Lyu Y, Meng X. Assessment of sugar content, fatty acids, free
666 amino acids, and volatile profiles in jujube fruits at different ripening stages. Food Chem.
667 2019; 270:344–52; doi:10.1016/j.foodchem.2018.07.102.
668 [31] Hong X, Wang J, Qi G. E-nose combined with chemometrics to trace tomato-juice quality. J
669 Food Eng. 2015;149:38–43; doi:10.1016/j.jfoodeng.2014.10.003.
670 [32] Di Natale C, Martinelli E, D'Amico A. Counteraction of environmental disturbances of
671 electronic nose data by independent component analysis. Sensors Actuators B Chem.
672 2002;82(2–3):158–65; doi:10.1016/S0925-4005(01)01001-2.
673 [33] Buttery R, Teranishi R, Ling LC. Fresh tomato aroma volatiles: A quantitative study. J Agric
674 Food Chem. 1987;35(4):540–4.
675 [34] Tieman D, Bliss P, McIntyre LM, Blandon-Ubeda A, Bies D, Odabasi AZ, et al. The chemical
676 interactions underlying tomato flavor preferences. Curr Biol. 2012;22(11):1035–9; doi:
677 10.1016/j.cub.2012.04.016.
678 [35] Padilla M, Perera a., Montoliu I, Chaudry a., Persaud K, Marco S. Drift compensation of gas
679 sensor array data by Orthogonal Signal Correction. Chemom Intell Lab Syst. 2010;100(1):28–
680 35; doi:10.1016/j.chemolab.2009.10.002.

681 [36] Tomic O, Ulmer H, Haugen JE. Standardization methods for handling instrument related signal
682 shift in gas-sensor array measurement data. Anal Chim Acta. 2002;472(1–2):99–111; doi:
683 10.1016/S0003-2670(02)00936-4.
684 [37] Tomic O, Eklöv T, Kvaal K, Haugen JE. Recalibration of a gas-sensor array system related to
685 sensor replacement. Anal Chim Acta. 2004;512(2):199–206; doi: 10.1016/j.aca.2004.03.001.
686 [38] Zhang L, Zhang D. Domain Adaptation Extreme Learning Machines for Drift Compensation
687 in E-Nose Systems. IEEE Trans Instrum Meas. 2015;64(7):1790–801; doi:
688 10.1109/TIM.2014.2367775.
689 [39] Yan K, Zhang D. Calibration transfer and drift compensation of e-noses via coupled task
690 learning. Sensors Actuators, B Chem. 2016;225:288–97; doi:10.1016/j.snb.2015.11.058.
691 [40] Solórzano A, Rodríguez-Pérez R, Padilla M, Graunke T, Fernandez L, Marco S, et al. Multi-
692 unit calibration rejects inherent device variability of chemical sensor arrays. Sensors Actuators,
693 B Chem. 2018;265:142–54; doi:10.1016/j.snb.2018.02.188.
694 [41] Ziyatdinov A, Marco S, Chaudry A, Persaud K, Caminal P, Perera A. Drift compensation of
695 gas sensor array data by common principal component analysis. Sensors Actuators, B Chem.
696 2010;146(2):460–5; doi:10.1016/j.snb.2009.11.034.
697 [42] Fernandez L, Guney S, Gutierrez-Galvez A, Marco S. Calibration transfer in temperature
698 modulated gas sensor arrays. Sensors Actuators, B Chem. 2016;231:276–84;
699 doi:10.1016/j.snb.2016.02.131.
700 [43] Gutierrez-Osuna R. Drift reduction for metal-oxide sensor arrays using canonical correlation
701 regression and partial least squares. Proc 7th Int Symp Olfaction Electron Nose. 2000;1–7.
702 [44] Vergara A, Vembu S, Ayhan T, Ryan MA, Homer ML, Huerta R. Chemical gas sensor drift
703 compensation using classifier ensembles. Sensors Actuators, B Chem. 2012;166–167:320–9;
704 doi:10.1016/j.snb.2012.01.074.
705 [45] Cebolla-Cornejo J, Roselló S, Valcárcel M, Serrano E, Beltrán J, Nuez F. Evaluation of
706 genotype and environment effects on taste and aroma flavour components of Spanish fresh

707 tomato. J Agric Food Chem. 2011;59:2440–50; doi: 10.1021/jf1045427.
708 [46] Cebolla-Cornejo J, Soler S, Nuez F. Genetic erosion of traditional varieties of vegetable
709 crops in Europe: tomato cultivation in Valencia (Spain) as a case Study. Int J Plant Prod.
710 2007;1(2):113–28.

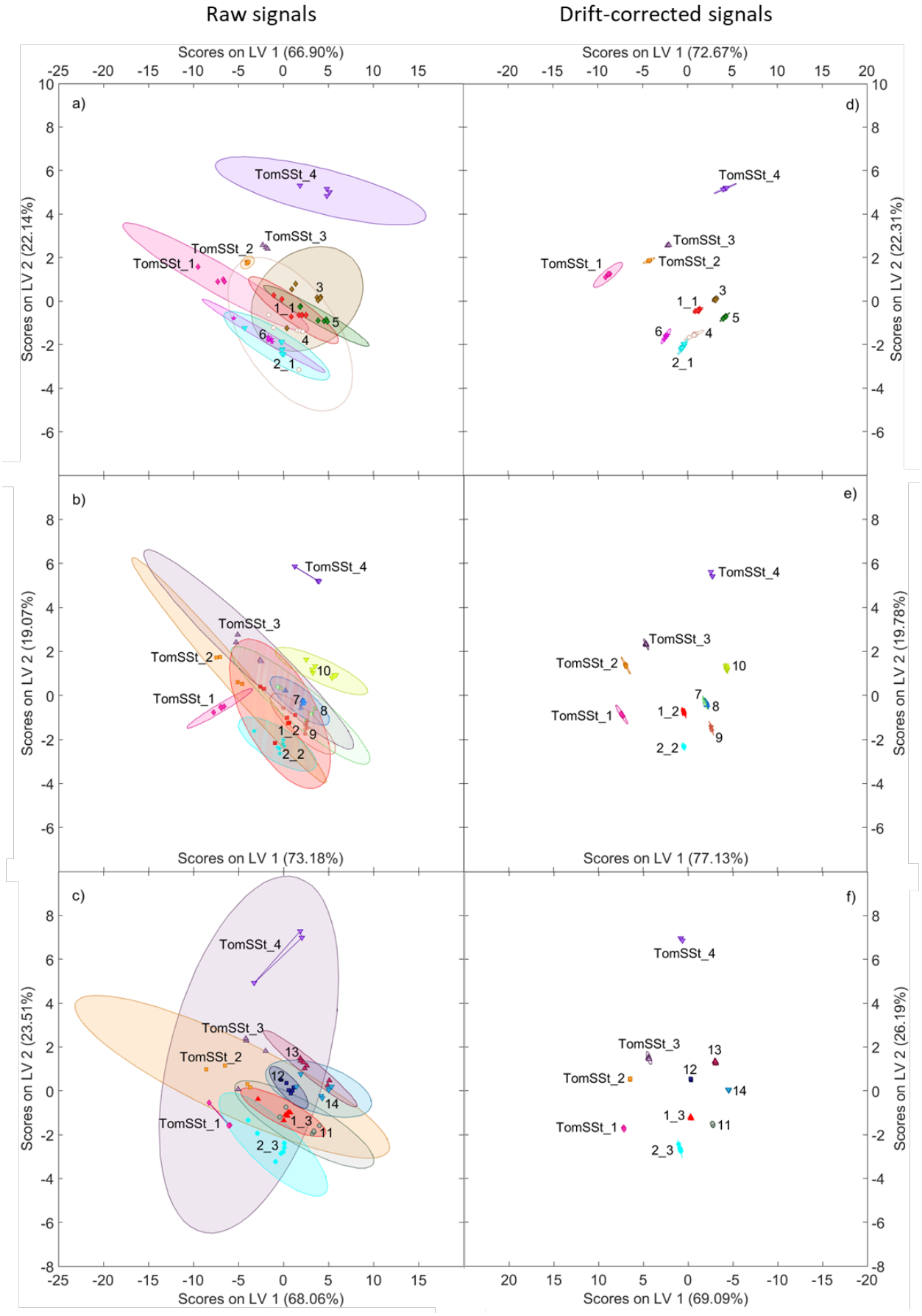
Raw signals
Drift-corrected signals
a)
b)
c)
d)
e)
f)
Scores on LV 1 (66.90%)
Scores on LV 2 (22.14%)
Scores on LV 1 (73.18%)
Scores on LV 2 (19.07%)
Scores on LV 1 (68.06%)
Scores on LV 2 (23.51%)
Scores on LV 1 (72.67%)
Scores on LV 2 (22.31%)
Scores on LV 1 (77.13%)
Scores on LV 2 (19.78%)
Scores on LV 1 (69.09%)
Scores on LV 2 (26.19%)
TomSSt_1
TomSSt_2
TomSSt_3
TomSSt_4

Fig. 1

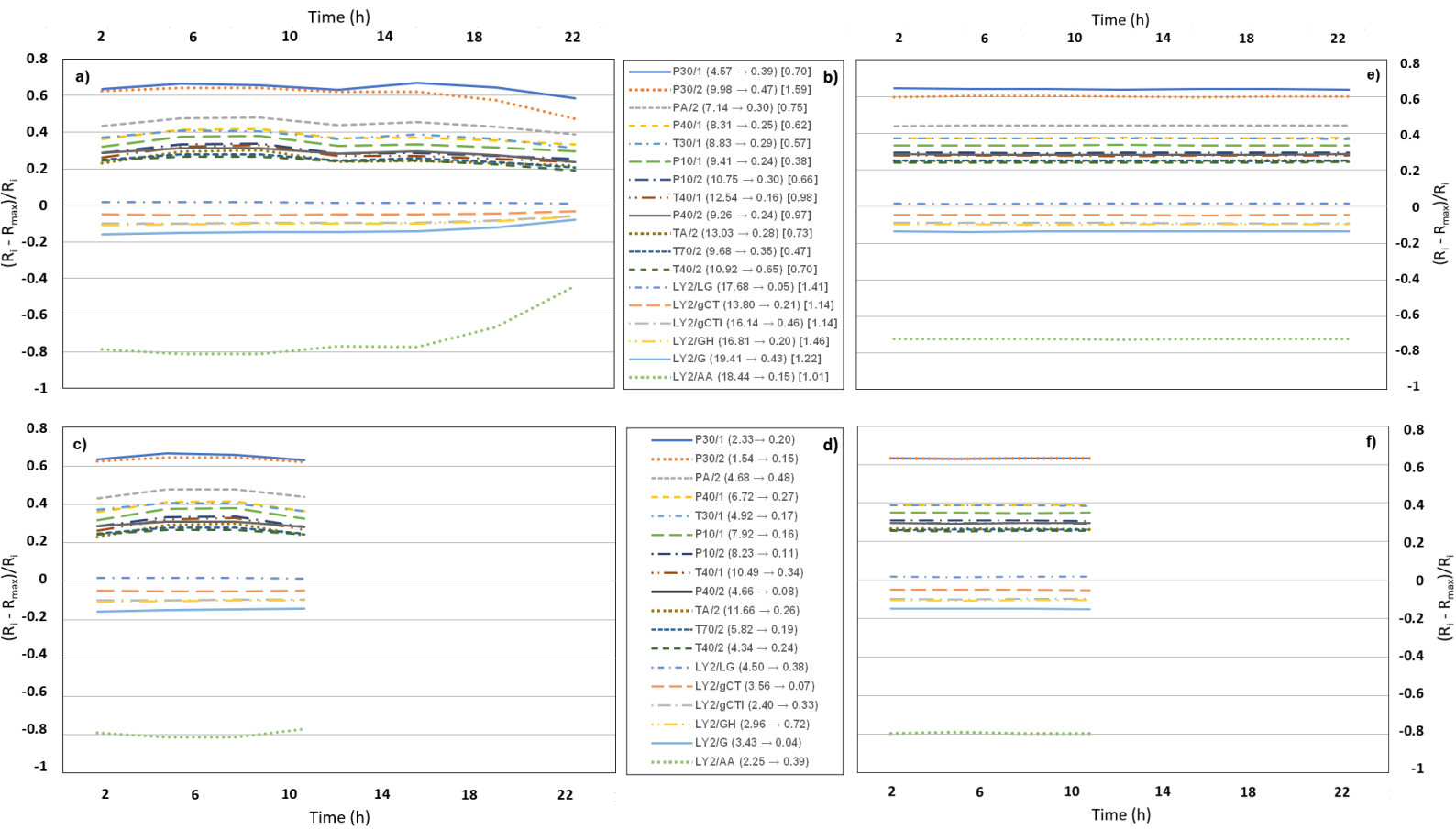
a)
b)
c)
d)
e)
f)
Time (h)
(Ri - Rmax)/Ri
P30/1 (4.57 → 0.39) [0.70]
P30/2 (9.98 → 0.47) [1.59]
PA/2 (7.14 → 0.30) [0.75]
P40/1 (8.31 → 0.25) [0.62]
T30/1 (8.83 → 0.29) [0.57]
P10/1 (9.41 → 0.24) [0.38]
P10/2 (10.75 → 0.30) [0.66]
T40/1 (12.54 → 0.16) [0.98]
P40/2 (9.26 → 0.24) [0.97]
TA/2 (13.03 → 0.28) [0.73]
T70/2 (9.68 → 0.35) [0.47]
T40/2 (10.92 → 0.65) [0.70]
LY2/LG (17.68 → 0.05) [1.41]
LY2/gCT (13.80 → 0.21) [1.14]
LY2/gCTI (16.14 → 0.46) [1.14]
LY2/GH (16.81 → 0.20) [1.46]
LY2/G (19.41 → 0.43) [1.22]
LY2/AA (18.44 → 0.15) [1.01]
P30/1 (2.33→ 0.20)
P30/2 (1.54 → 0.15)
PA/2 (4.68 → 0.48)
P40/1 (6.72 → 0.27)
T30/1 (4.92 → 0.17)
P10/1 (7.92 → 0.16)
P10/2 (8.23 → 0.11)
T40/1 (10.49 → 0.34)
P40/2 (4.66 → 0.08)
TA/2 (11.66 → 0.26)
T70/2 (5.82 → 0.19)
T40/2 (4.34 → 0.24)
LY2/LG (4.50 → 0.38)
LY2/gCT (3.56 → 0.07)
LY2/gCTI (2.40 → 0.33)
LY2/GH (2.96 → 0.72)
LY2/G (3.43 → 0.04)
LY2/AA (2.25 → 0.39)

Fig. 2

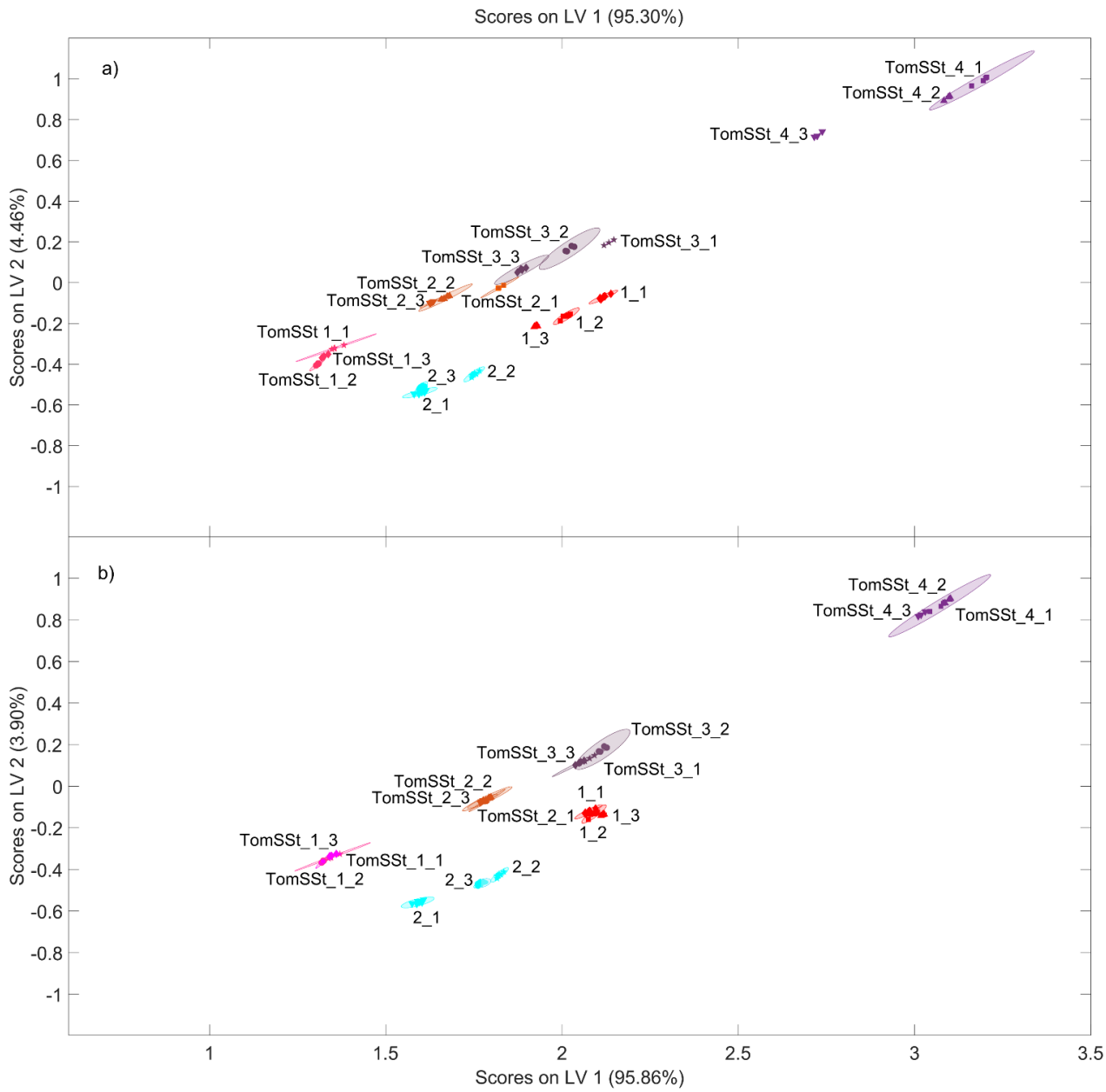
Scores on LV 1 (95.30%)
a)
Scores on LV 2 (4.46%)
TomSSt_4_1
TomSSt_4_2
TomSSt_4_3
TomSSt_3_2
TomSSt_3_1
TomSSt_3_3
TomSSt_2_2
TomSSt_2_3
TomSSt_2_1
1_1
1_2
1_3
TomSSt 1_1
TomSSt_1_3
TomSSt_1_2
2_3
2_2
2_1
b)
Scores on LV 2 (3.90%)
TomSSt_4_2
TomSSt_4_3
TomSSt_4_1
TomSSt_3_2
TomSSt_3_3
TomSSt_3_1
TomSSt_2_2
TomSSt_2_3
1_1
TomSSt_2_1
1_3
1_2
TomSSt_1_3
TomSSt_1_1
TomSSt_1_2
2_3
2_2
2_1
Scores on LV 1 (95.86%)

Fig. 3

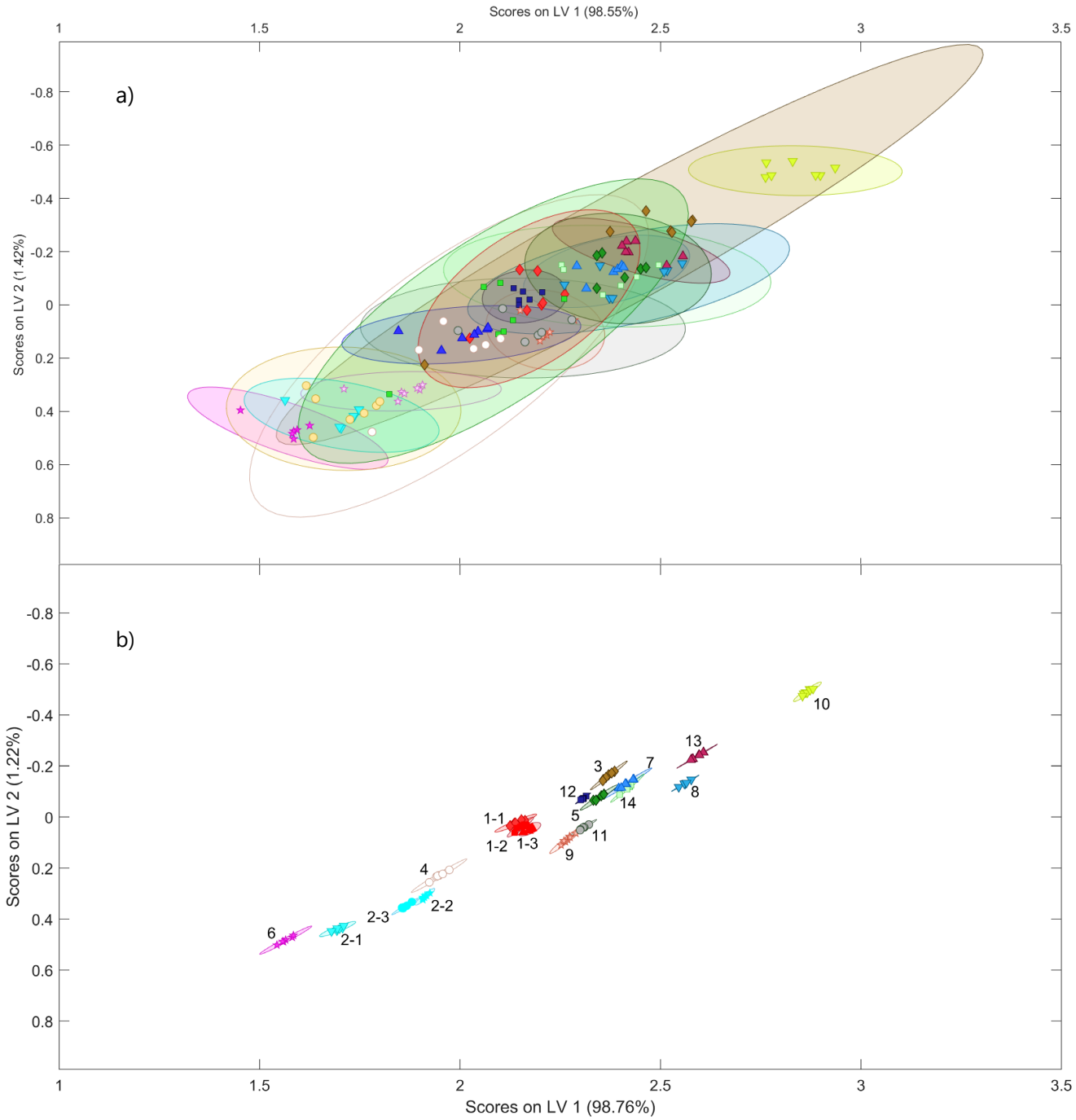
Scores on LV 1 (98.55%)
a)
Scores on LV 2 (1.42%)
b)
Scores on LV 2 (1.22%)
Scores on LV 1 (98.76%)
10
13
3
7
12
8
14
5
1-1
11
1-2
1-3
9
4
2-2
2-3
6
2-1

Fig. 4

Supp. Fig. 1. Schematic representation of short-term drift within a sequence.

1.- Getting raw data from e-nose

			Sensors response							
Injection nº	**Sample**	**Injection time (h)**	**LY2/LG**	**LY2/G**	**LY2/AA**	**LY2/Gh**	**LY2/gCTI**	**LY2/gCT**	**T30/1**	**…**
1	TomSST 2	0,00	0,667	-2,17	-2,06	-2,03	-2,03	-0,905	0,817	…
2	3	0,35	0,146	-0,477	-0,554	-0,384	-0,295	-0,113	0,649	…
3	6	0,70	0,106	-0348	-0,428	-0,273	-0,203	-0,079	0,622	…
4	2_1	1,03	0,392	-0,528	-0,64	-0,403	-0,301	-0,104	0,645	…
…	…	…	…	…	…	…	…	…	…	…

2.- Appliying multiplicative pretreatment for each sample class

$$S = \left(\frac{S_{i_{(j)},k\ \text{measured}}}{\hat{S}_{i,k\ \text{measured}}}\right)$$

Eg.: $$\text{LY2/LG}_{\ \text{TomSST2 injection 1}} = \left(\frac{0{,}667}{\hat{S}_{TomSST2\ class}}\right) = \left(\frac{0{,}667}{0{,}643}\right)$$

3.- Performing PLS regression to model intra-sequence drift (in PLSToolbox for Matlab)

Y = Injection time (h) (n x 1 vector)
X = Pretreated sensor response matrix (n samples x 18 sensor matrix)

(Outliers removed from the model based on Q residuals and T2 Hotelling statistics if necessary)

4.- Obtaining intra-sequence drift (in Matlab)

Obtaining scores and loadings matrices from de PLS model
(extracting data from de model as raw data)

Scores (matrix of n samples x number of latent variables selected)
Loadings (matrix of 18 sensors x number of latent variables selected)

Intra-sequence **drift** matrix (E_{drift})= scores * loadings‘

(matrix product in Matlab command window giving a n samples x 18 sensors matrix)

5.- Substracting intra-sequence drift from raw data signal (in Matlab or Excel)

$$S_{i_{(j)},k\ \text{corrected}} = [\hat{S}_{i,k\ \text{measured}}(1 - E_{i_{(j)},k\ \text{drift}}\ (t))] + S_{i_{(j)},k\ \text{measured}}$$

Eg.: $$\text{LY2/LG}_{\ \text{TomSST2 injection 1 corrected}} = 0{,}643\ (1\text{- }E_{\text{drift }1,1}) + 0{,}667 = 0{,}6419$$

Supp. Fig. 2. Schematic representation of long-term drift with several sequences.

1.- Getting raw data from e-nose for each sequence

Seq matrix 1 | Seq matrix 2 | ... | Seq matrix m

2.- Performing intra-sequence drift correction for each sequence data matrix

Seq matrix 1 intra-seq corrected | Seq matrix 2 intra-seq corrected | ... | Seq matrix m intra-seq corrected

3.- Appliying multiplicative pretreatment for each sample class

$$\frac{S_{i_{(j)},k\ measured}}{\hat{S}_{i,k\ measured}+(\hat{S}_{TomSSt1,k}-\hat{S}_{TomSStn,k})}$$

Eg.: $$\text{LY2/LG}_{\text{TomSST2 injection 1 seq 2}} = \left(\frac{S_{1,1\ TomSST2}}{\widehat{S_{TomSST2\ class\ seq\ 1}} - S_{TomSST2\ class\ seq\ 2}}\right) = \left(\frac{0{,}652}{0{,}643 - 0{,}627}\right)$$

Seq matrix 1 intra-seq corrected | Seq matrix 2 intra-seq corrected + multiplicative pretreated | ... | Seq matrix m intra-seq corrected + multiplicative pretreated

4.- Performing PLS regression to model inter-sequence drift with all corrected matrices joined (in PLSToolbox for Matlab)

Y vector
(injection time in hous; continuous for the whole trial)

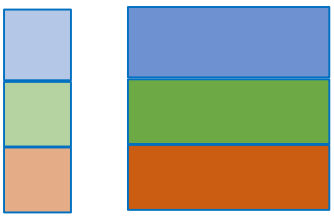

X matrix
(sensor signals)

5.- Obtaining inter-sequence drift (in Matlab)

6.- Substracting intra-sequence drift from raw data signal (in Matlab or Excel)

→ Similar as described for intra-sequence drift correction